Supporting Information

Facile synthesis of PdSn alloy octopods through Stranski-Krastanov growth mechanism as electrocatalysts towards ethanol oxidation reaction

Jingbo Huang,‡[a] Liang Ji,‡[a] Xiao Li,[a] Xingqiao Wu,[a] Ningkang Qian,[a] Junjie Li,[a] Yucong Yan,[a,c] Deren Yang[a] and Hui Zhang[a,b,*]

[a]State Key Laboratory of Silicon Materials and School of Materials Science and Engineering, Zhejiang University, Hangzhou, Zhejiang 310027, People's Republic of China. E-mail: msezhanghui@zju.edu.cn.

[b]Institute of Advanced Semiconductors, Hangzhou Innovation Center, Zhejiang University, Hangzhou, Zhejiang 310027, People's Republic of China.

[c]BTR New Material Group CO., LTD., GuangMing District, Shenzhen 518106, People's Republic of China.

‡ These authors contributed equally to this work.

DFT calculation

Density functional theory (DFT) calculations were performed using CASTEP package with the Perdew-Burke-Ernzerhof (PBE) generalized gradient approximation (GGA) exchange-correlation functional.[1,2] Five layers of 5×5 Pd (100), PdSn with Sn mole percentage of 6% and 28%, all of which contain 125 atoms were chosen as the slab model, and a vacuum region with 15 Å was set to create the truly two-dimensional (100) surface.

The Ultrosoft Pseudopotentials were used to describe the ionic core electrons, and a plane-wave basis set with a cutoff energy of 300 eV was adopted to treat the valence electrons. A threshold of self-consistent-field energy convergence was $1x10^{-5}$ eV/atom, and the maximum force and displacement of the convergence criterion for the structural optimizations were set to 0.03 eV/Å and 0.001 Å, respectively.

The adsorption energy (E_{ads}) is calculated according to the formula:

$$E_{ads} = E_{\mathrm{CH3CO}-catalyst} - (E_{\mathrm{CH3CO}} + E_{catalyst}) \quad (1)$$

in which $E_{\mathrm{CH3CO}-catalyst}$ is the calculated total energy of the system with CH_3CO adsorbed on various (100) surfaces; E_{CH3CO} represents the energy of isolated CH_3CO; and $E_{catalyst}$ is the energy of (100) faceted Pd or PdSn catalyst. A more negative E_{ads} in equation (1) implies that the adsorption is thermodynamically more favorable.

References

1 K. Gundersen, B. Hammer, K. W. Jacobsen, J. K. Nørskov, J. S. Lin and V. Milman, Surf. Sci., 1993, 285, 27-30.

2 J. P. Perdew, K. Burke and M. Ernzerhof, Phys. Rev. Lett., 1996, 77, 3865-3868.

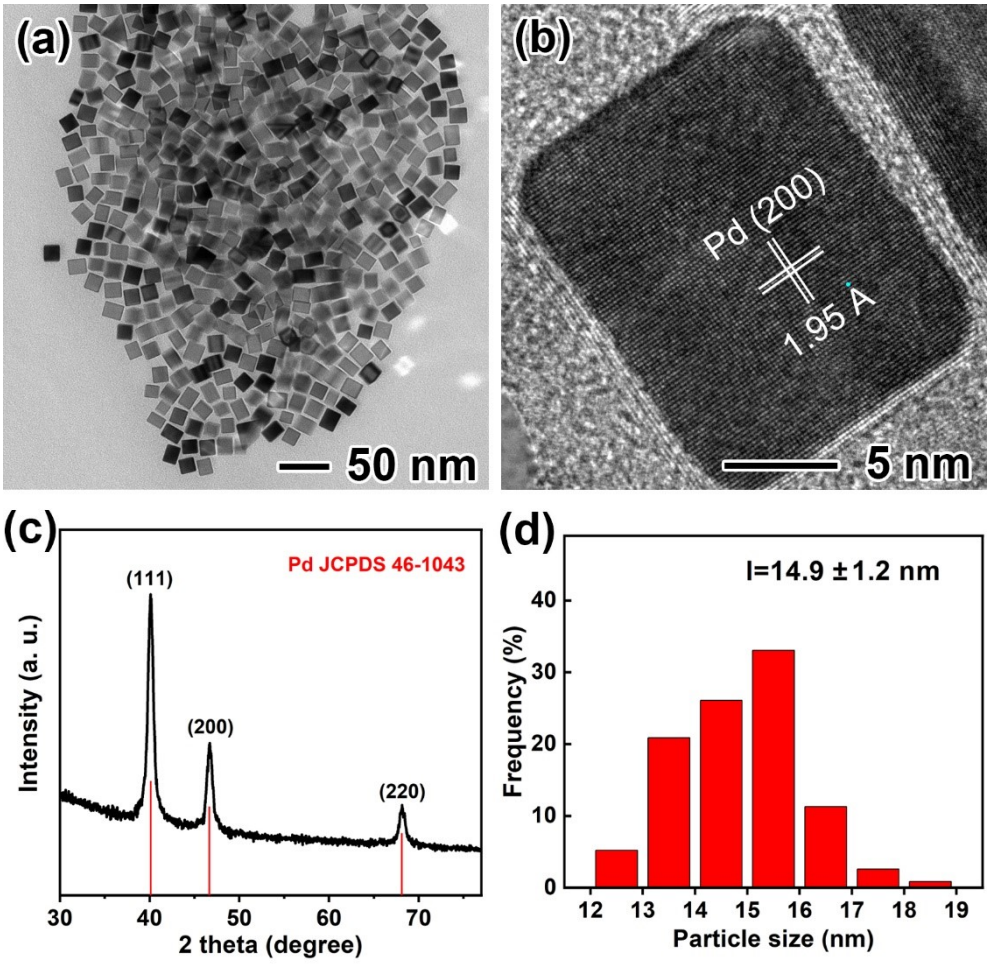

Figure S1. Morphological, structural, and size characterizations of Pd cubes. (a) TEM image, (b) HRTEM image, (c) XRD pattern, and (d) histogram of size distribution. The size of cubes is defined as the distance between two opposite faces.

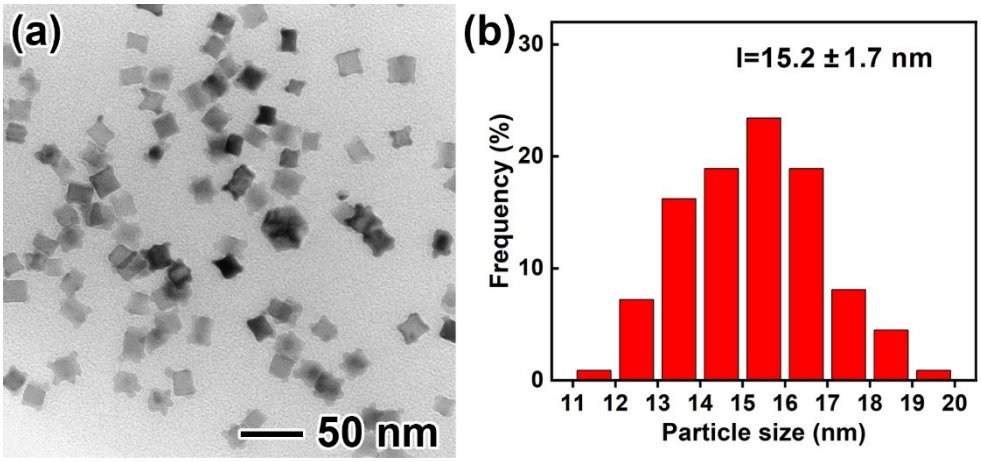

Figure S2. Morphological and size characterizations of $Pd_{87}Sn_{13}$ octopods. (a) TEM image and (b) histogram of size distribution. The size of octopods is defined as the distance between two opposite faces.

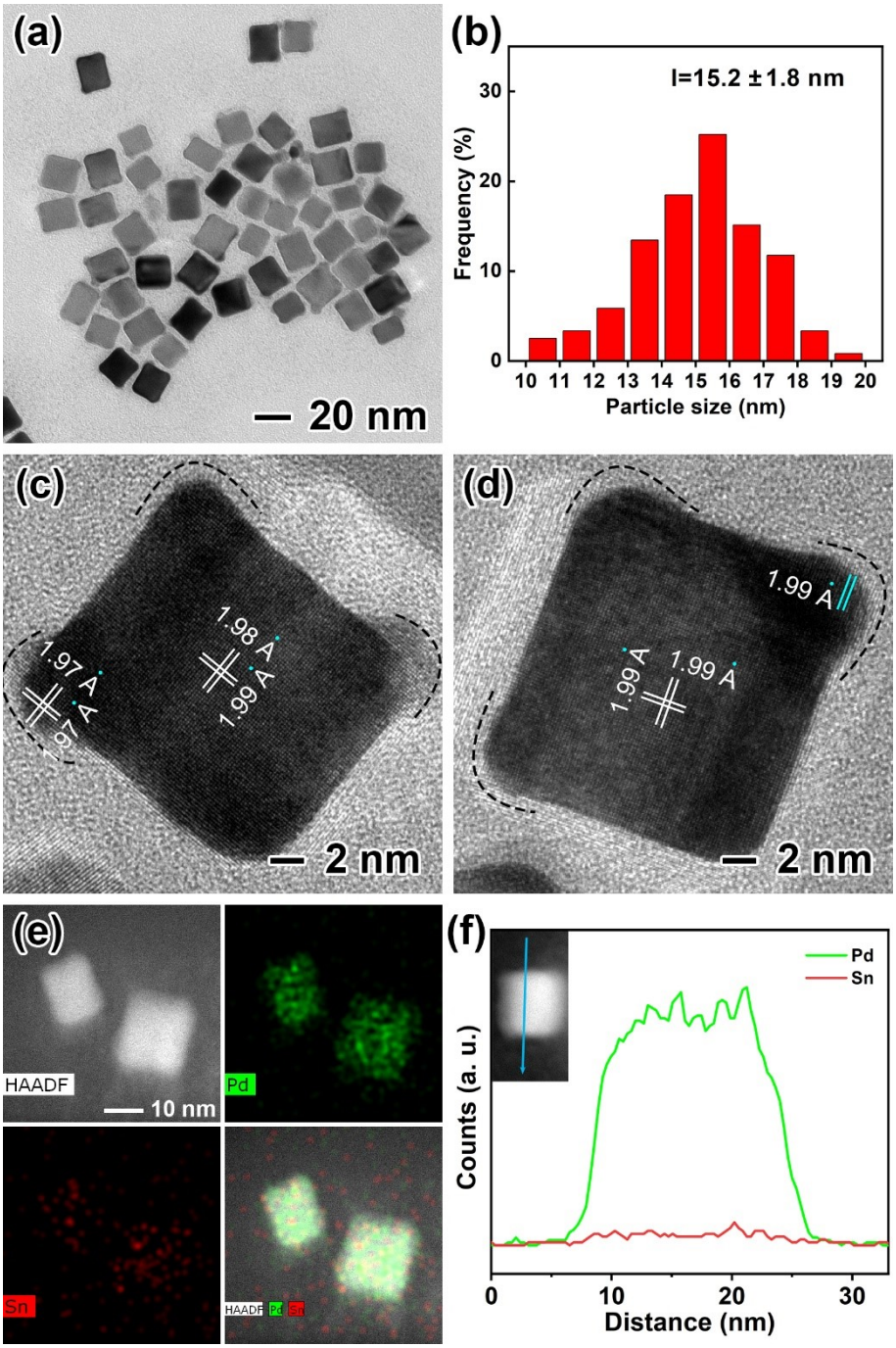

Figure S3. Morphological, structural, and compositional characterizations of the $Pd_{94}Sn_6$ nanocrystals. (a) TEM image, (b) histogram of size distribution, (c, d) HRTEM images, (e) EDX-mapping image, and (f) EDX line-scan analysis. The size of octopods is defined as the distance between two opposite faces.

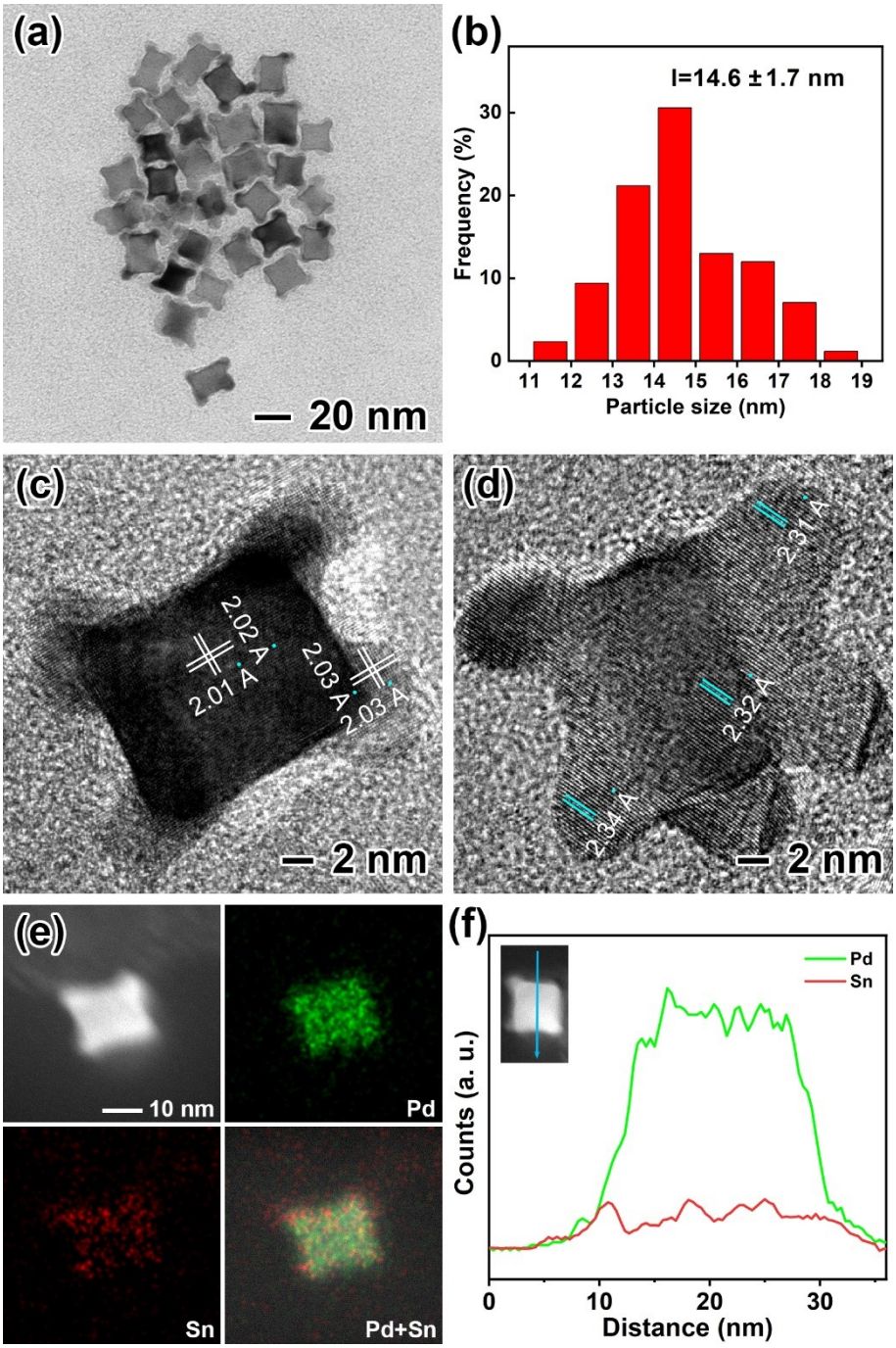

Figure S4. Morphological, structural, and compositional characterizations of the $Pd_{72}Sn_{28}$ octopods. (a) TEM image, (b) histogram of size distribution, (c, d) HRTEM images, (e) EDX-mapping image, and (f) EDX line-scan profiles. The size of octopods is defined as the distance between two opposite faces.

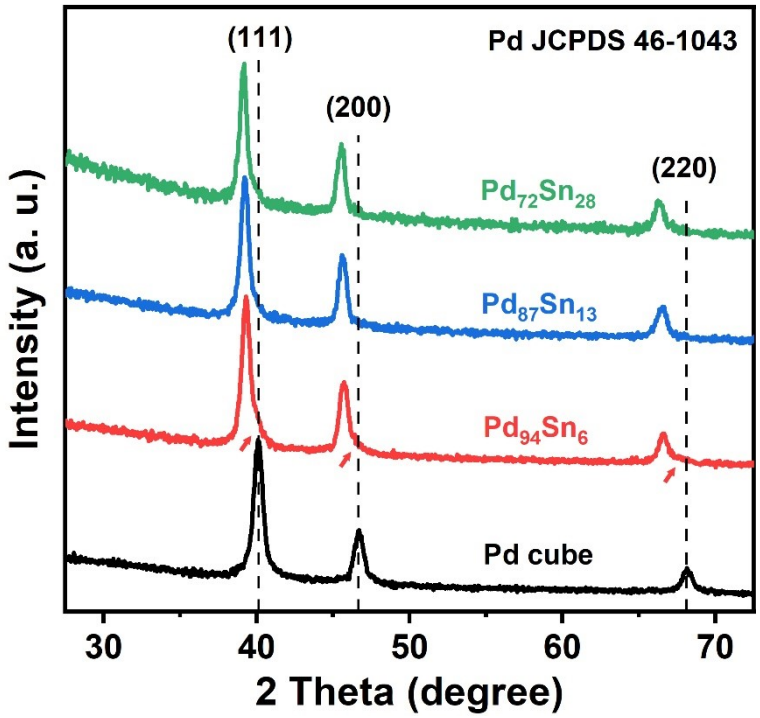

Figure S5. XRD patterns of PdSn alloy nanocrystals with different compositions.

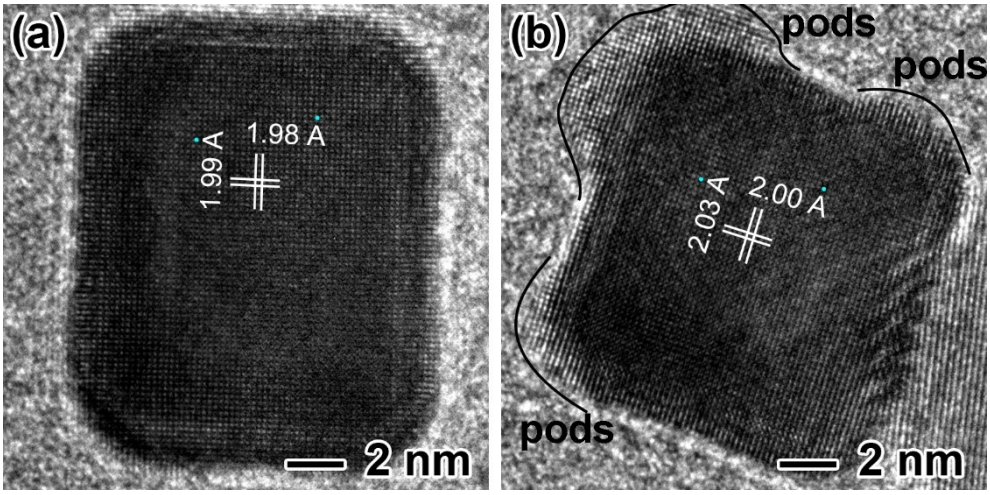

Figure S6. HRTEM images of the PdSn octopods synthesized at 200 ℃ at (a) 1 h and (b) 2.5 h.

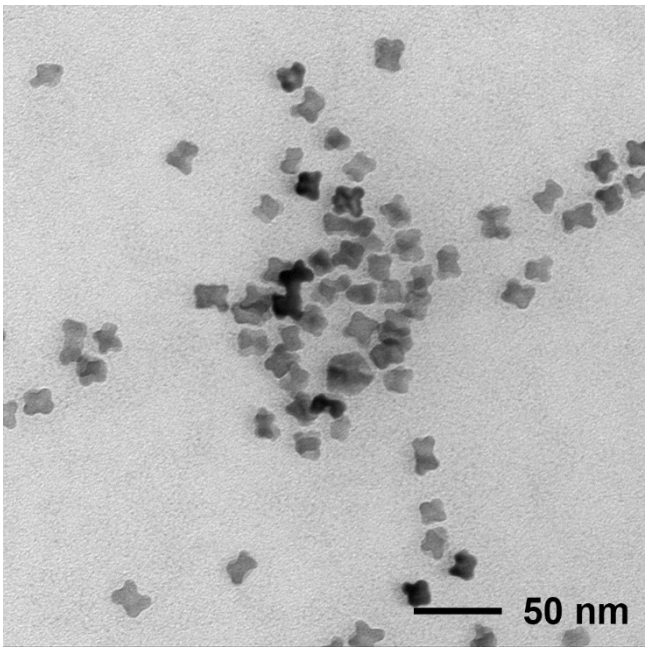

Figure S7. TEM image of the PdSn octopods synthesized at 200 ℃ for 5 h.

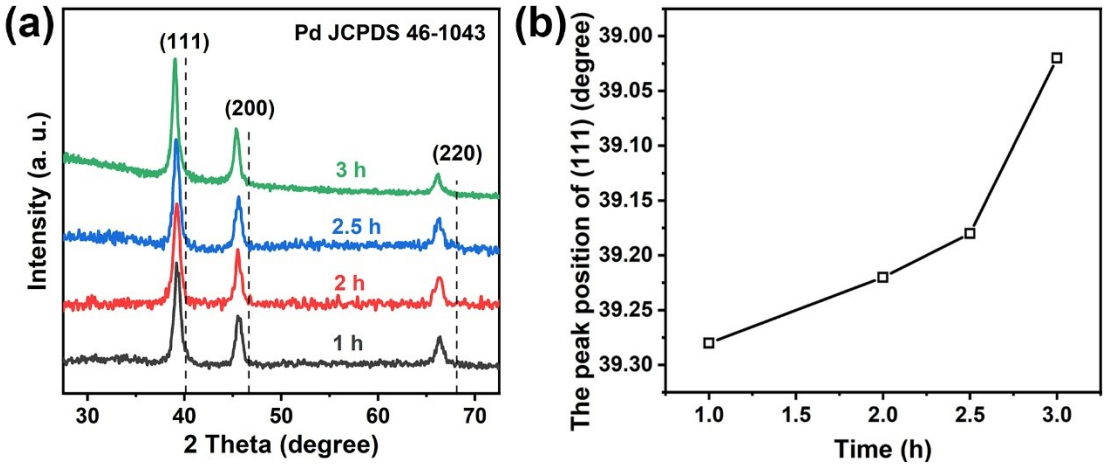

Figure S8. (a) Time-evolution XRD patterns of the PdSn octopods synthesized at 200 ℃, and (b) the fine variation of the peak position of {111} planes in (a).

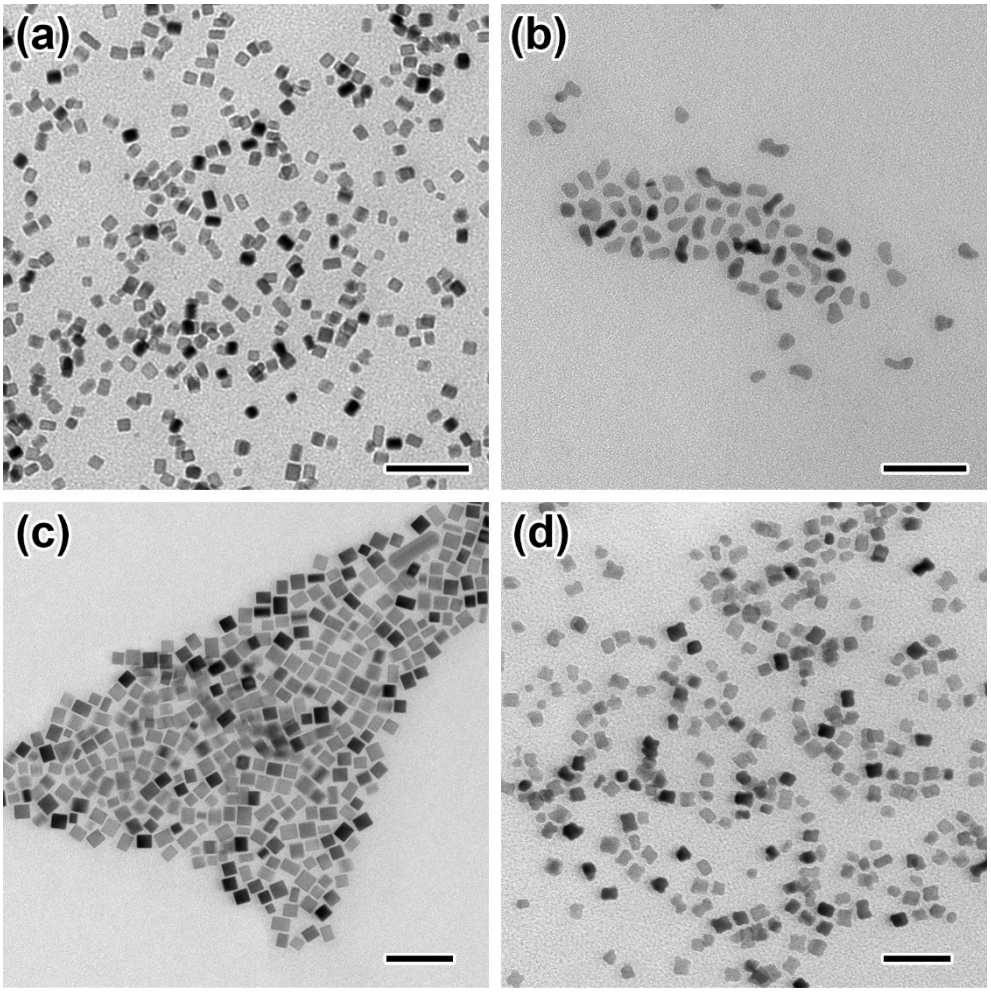

Figure S9. TEM images of the PdSn nanocrystals using Pd cubes with different sizes as seeds: (a) 6 nm Pd cubes, (b) PdSn nanocrystals using 6 nm Pd cubes as seeds, (c) 10 nm Pd cubes, and (d) PdSn octopods nanocrystals using 10 nm Pd cubes as seeds. Scale bars are 50 nm.

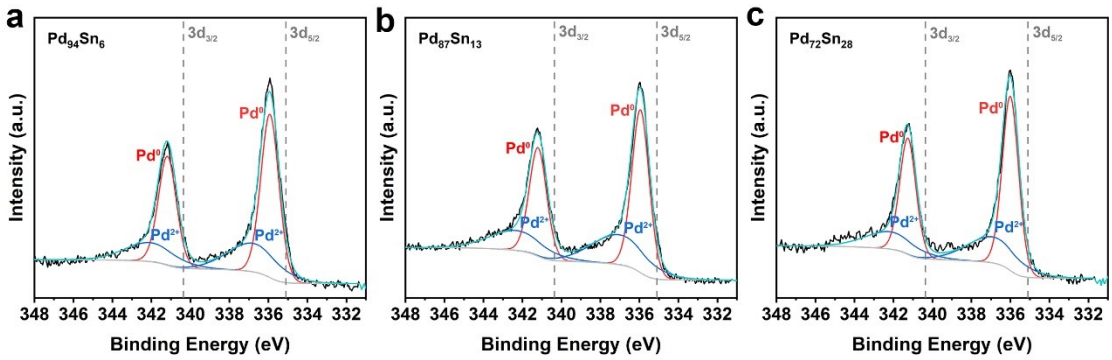

Figure S10. Pd 3d XPS spectra of (a) $Pd_{94}Sn_6$, (b) $Pd_{87}Sn_{13}$, and (c) $Pd_{72}Sn_{28}$ octopods.

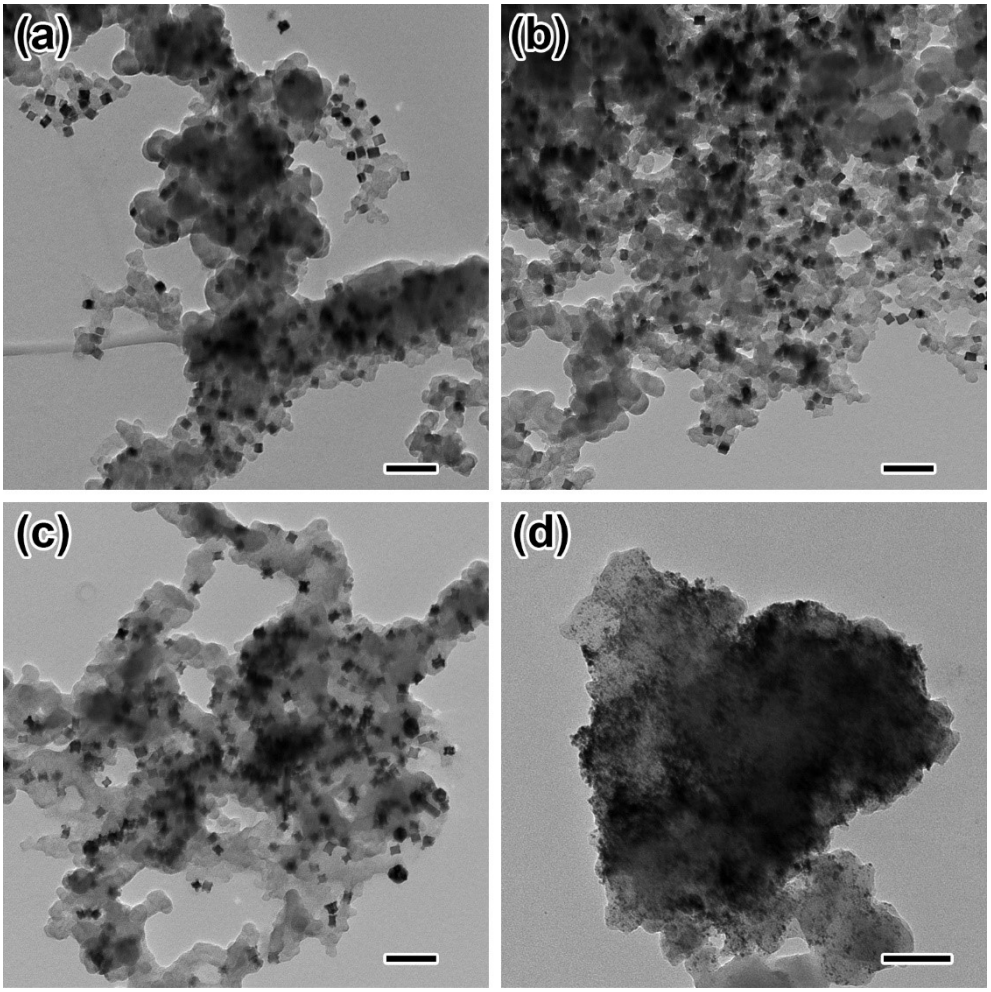

Figure S11. TEM images of carbon-loaded (a) $Pd_{94}Sn_6$, (b) $Pd_{87}Sn_{13}$, (c) $Pd_{72}Sn_{28}$, and (d) commercial Pd/C. Scale bars are 100 nm.

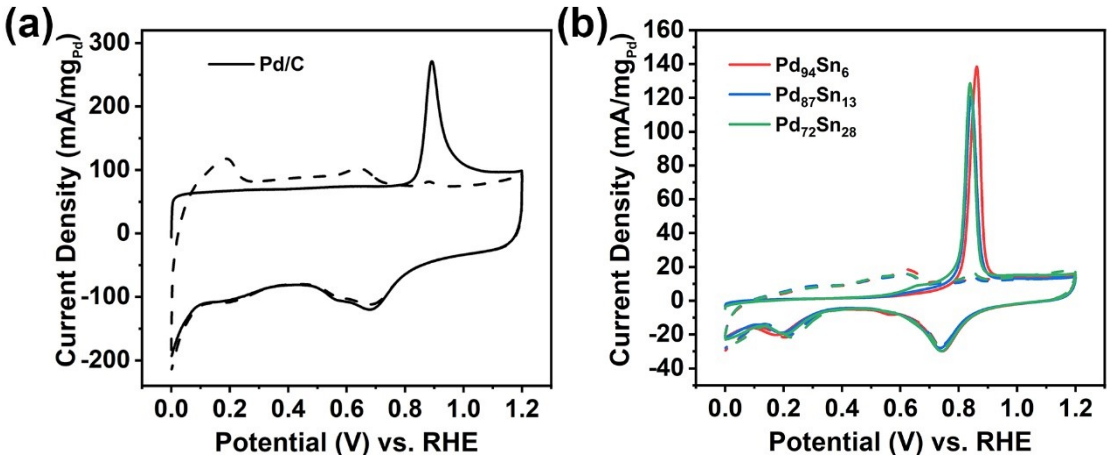

Figure S12. CO stripping voltammograms of (a) commercial Pd/C and (b) PdSn alloy catalysts with different compositions in 1 M KOH solution normalized to the mass of Pd.

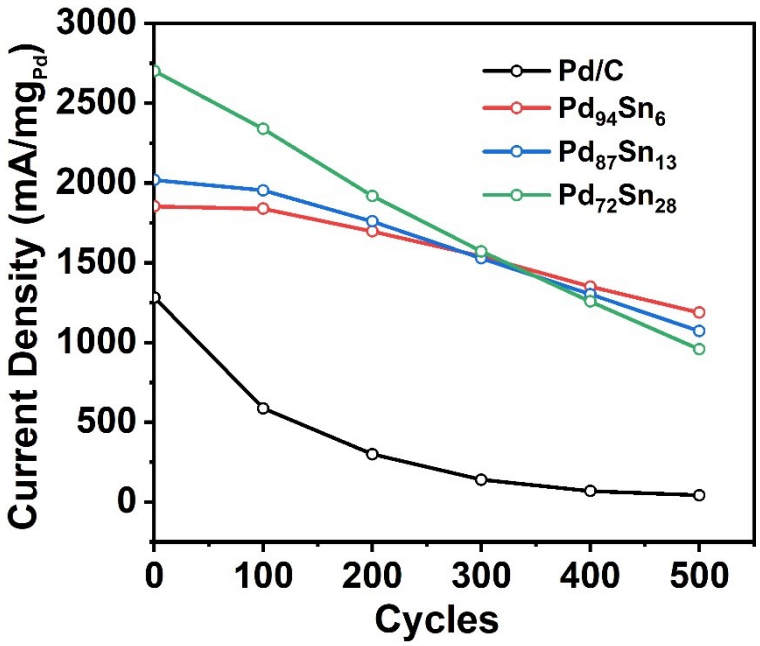

Figure S13. EOR cycling stability curves of all the catalysts normalized to the mass of Pd.

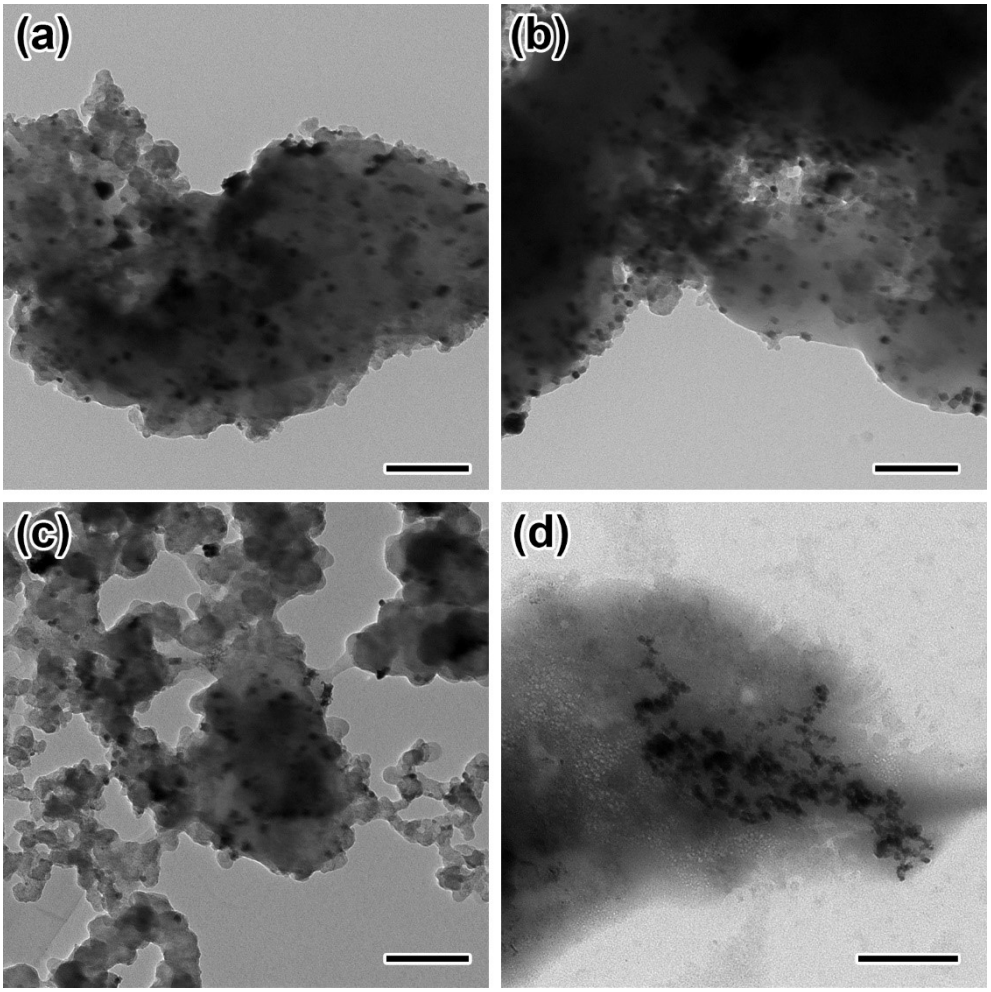

Figure S14. TEM images of carbon-loaded (a) $Pd_{94}Sn_6$, (b) $Pd_{87}Sn_{13}$, (c) $Pd_{72}Sn_{28}$, and (d) commercial Pd/C after stability tests. Scale bars are 200 nm.

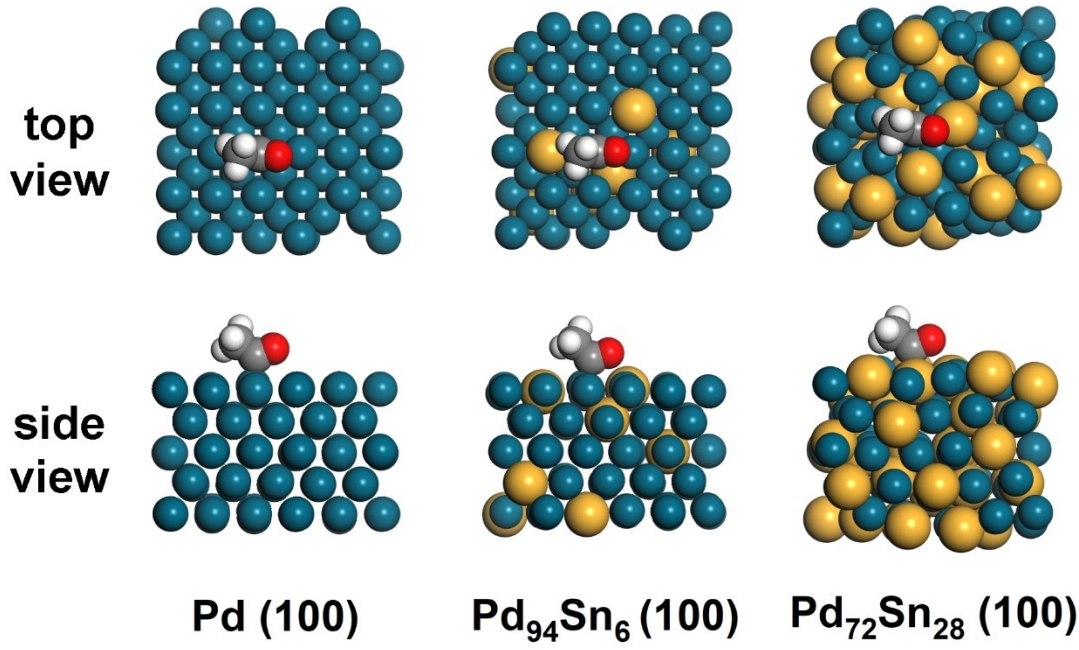

Figure S15. DFT calculation models of Pd (100), $Pd_{94}Sn_6$ (100), and $Pd_{72}Sn_{28}$ (100) together with configurations of $*CH_3CO$. The cyan, yellow, gray, white, and red balls are corresponding to Pd, Sn, C, H, and O atoms, respectively.